Instruments and Experimental Techniques, Vol. 42, No. 1, 1999, pp. 94–99. Translated from Pribory i Tekhnika Eksperimenta, No. 1, 1999, pp. 105–111.
Original Russian Text Copyright © 1999 by Tur'yanskii, Vinogradov, Pirshin.

GENERAL EXPERIMENTAL TECHNIQUES

A Two-Wave X-ray Reflectometer

A. G. Tur'yanskii, A. V. Vinogradov, and I. V. Pirshin

Lebedev Institute of Physics, Russian Academy of Sciences, Leninskii pr. 53, Moscow, 117924 Russia

Received June 30, 1998

Abstract—A new scheme of a two-wave X-ray reflectometer with a beamsplitter made of semitransparent plates of pyrolytic graphite is proposed. When tuned to the CuK_α characteristic line, the beamsplitter has a peak reflectivity of 22% and transparency of 85% for the CuK_β line. The reflectometer arrangement provides simultaneous data collection in two spectral bands and self-calibration in relative measurements. This allows for a sharp increase in measurement accuracy and sensitivity. Results of measurements of a multilayer Ni–C structure and a single-crystal GaAs film are presented.

Two- or three-crystal spectrometers, which are adapted for measurements at grazing incidence angles of the probe X-ray beam, usually form the measurement base of X-ray reflectometers. Such versions of the measurement arrangement are used when working with standard X-ray tubes [1, 2] and synchrotron sources [3]. A common drawback of the aforementioned schemes is the laborious adjustment of the X-ray channel and the goniometric arrangemeent when changing to another operating X-ray spectrum region. Their typical feature is the appearance of uncontrollable errors caused by a change in the geometrical parameters of the arrangement.

At the same time, a change to another probe radiation wavelength is necessary for obtaining more complete and unambiguous information on the structure and composition of thin-film structures and interfaces. The capabilities of solving this problem by using a polychromatic probe radiation source combined with a semiconductor detector [4] are limited by its insufficiently high energy resolution (200–250 eV). In addition, because of a low data-collection rate in a given spectral band, such a scheme has comparatively large statistical counting errors. This is determined by the necessity of detecting the full spectral region and by physical limitations for detector signal processing time.

This work describes a design of a two-wave reflectometer that provides simultaneous measurements in two spectral regions and comparatively simple tuning for other spectral regions. The constructed setup is a practical implementation of the measurement scheme proposed by us [5]. In this design, the required spectral lines are selected from the sample-scattered polychromatic radiation by semitransparent plates of pyrolytic graphite.

The basic advantage of this design is the possibility of performing relative measurements. As we show below, this allows one to eliminate or significantly reduce a number of principle errors of conventional one-wave reflectometry. Moreover, it becomes possible to obtain additional information on film and near-surface structures.

DESCRIPTION OF THE REFLECTOMETER

Figure 1 shows an X-ray optical diagram of the reflectometer. An ИРИС generator of X-ray radiation and a ГУР-8 goniometer served as the reflectometer's working platform. A БСВ-22 tube with a copper anode served as a radiation source. The dimensions of the visible projection of the X-ray focus were 8 × 0.04 mm. A special head for reflectometric measurements was

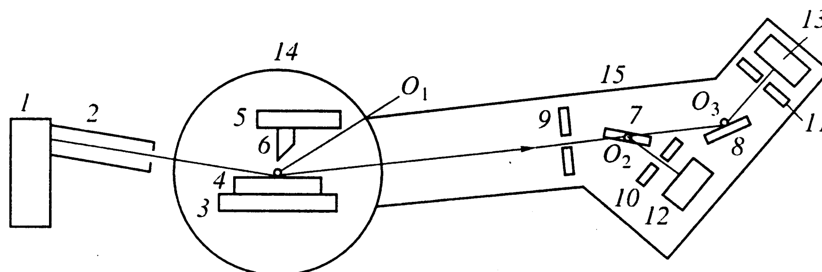

Fig. 1. Schematic drawing of the X-ray reflectometer: (*1*) X-ray tube; (*2*) collimator; (*3*) sample holder; (*4*) sample; (*5*) device for linear displacement of the shield; (*6*) absorbing shield; (*7*) semitransparent pyrographite monochromator; (*8*) replaceable monochromator; (*9–11*) slits; (*12, 13*) scintillation detectors; (*14*) rotating table of the goniometer; and (*15*) rotating cantilever.

0020-4412/99/4201-0094$22.00 © 1999 МАИК "Наука/Interperiodica"

placed on the principal axis of the goniometer. Holder *3*, which fixes the specified position of sample *4*, can move perpendicular to the X-ray beam axis within a distance of >70 mm, thus making it possible to measure samples in the form of rods with polished ends. A device for linear displacement *5* placed on the head controls the gap width between the absorbing shield *6* and the sample *4* surface with a step of 2.5 μm. The distances from the principal axis O_1 of the goniometer to the tube *1* focus and to the entrance slit diaphragm *9* were 330 and 225 mm, respectively. Elements *3–6* and *7–13* of the X-ray optical arrangement were placed on a rotating table *14* and on a rotating cantilever *15*, respectively.

A general view of the device for spectrum line selection and a diagram of the X-ray beam trajectory are shown in Fig. 2 in more detail. Rotating heads *16* and *17* of monochromators *7* and *8* are installed in holes of the supporting plate *18*. The latter can be displaced along the normal to the beam in two mutually perpendicular directions. The axes of rotation of supporting guides *19* and *20*, on which scintillation detectors are mounted, are aligned with the axes O_2 and O_3 of heads *16* and *17*.

The first monochromator on the X-ray beam path is a semitransparent plate of pyrolytic graphite with an area of 6 × 15 mm^2 and 46 μm thick. Hereafter, such elements of the X-ray optical arrangement are called semitransparent. Their transmittance is $T > 0.5$ in the working position for an arbitrary line in a given spectral band. The first monochromator was turned by an angle of 13.2° (the Bragg diffraction angle for the CuK_α line). Its peak reflectivity R_p for the CuK_α line and transmittance T for the CuK_β line were 0.22 and 0.85, respectively (Fig. 3). The half-width of the rocking curve at a fixed detector position is 0.49°.

The parameters of the second monochromator *8* are determined by the problem to be studied. In particular, Si or Ge single crystals can be selected for measuring the fine structure of interference maxima. When the second semitransparent plate and an additional detector are used as the second monochromator, we can measure signals at two spectral lines and simultaneously analyze the spectrum of the radiation transmitted through both monochromators (Fig. 2). The results presented below were obtained while adjusting the first and second monochromators at the CuK_α (0.154 nm) and CuK_β (0.139 nm) lines, respectively. The second monochromator was a 1-mm-thick pyrographite plate {with R_p(CuK_α) = 0.3} from the accessory set of a ДРОН-3М diffractometer. The use of two pyrographite monochromators allows for changes in the width of entrance slit *9*, providing the possibility of adjusting the selection angle when detecting the reflected radiation. Moreover, in this case, the tuning to another spectral line is simplified (e.g., for calibration of the both channels by CuK_β radiation).

The precise angular adjustment of monochromators is performed with a thin rod, of which one end is inserted into the rotating head and the other is fixed in the replaceable micrometer-feed unit. After the monochromators are adjusted for diffraction maxima of the the selected characteristic lines, the angular positions of the heads are fixed and the rods are removed.

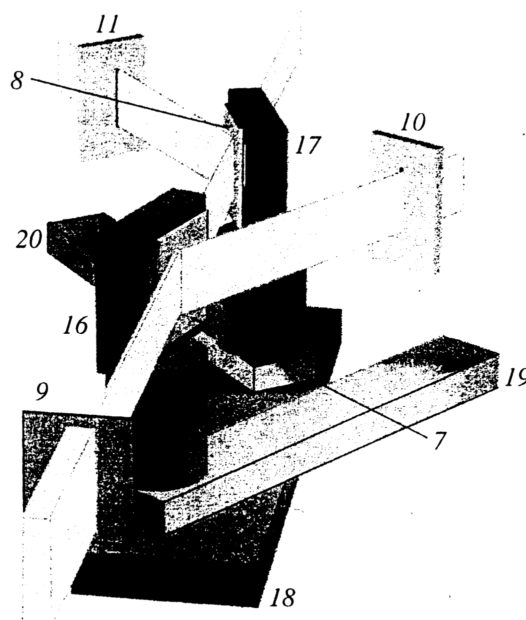

Fig. 2. Schematic diagram of beam splitting when passing through the device for selecting spectral lines (a design with two semitransparent monochromators): (*7*, *8*) semitransparent monochromators; (*9–11*) slits; (*16*, *17*) rotating heads; (*18*) base slab; and (*19*, *20*) supporting guides for detectors.

The control and data recording unit has a case measuring 33 × 30 × 13 cm (Evromekhanika standard). It consists of a power source, a Z80180 processor module, a stepper-motor control module, and two independent recording channels, each of which contains an amplitude discriminator and a PMT vottage source. The unit has its own memory of 128 Kbyte for storing the control program and collected data.

The experiment is planned in the interactive mode by using PC application software. Before the system starts operation, the description of the data acquisition conditions are loaded through an RS-232 interface into the control unit. Then, measurements are carried out autonomously under microprocessor control. When measurements are completed, the collected data are written in the PC memory and can be analyzed with standard visualization and digital processing programs.

A meander voltage generated by an optron (light-emitting diode–photodiode), which is built into the ГУР-8, was used as a signal of the angular position of the detector axis. The moments when the optron voltage begins to increase and decrease to specified levels were determined, thus providing a minimal synchronous angular displacement step of the sample and detector of

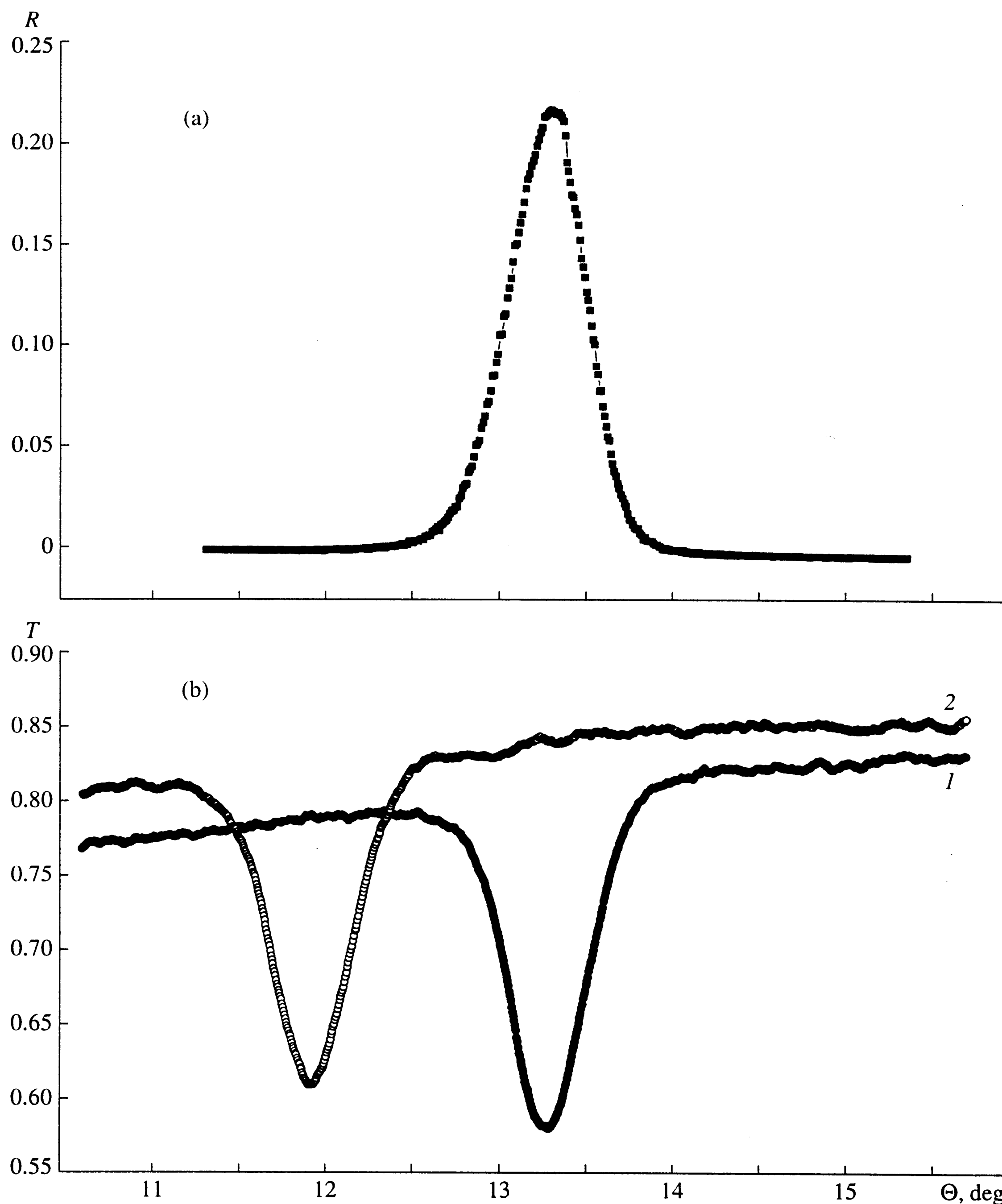

Fig. 3. Characteristics of the semitransparent pyrographite plate for Θ scanning: (a) the reflectivity $R(\Theta)$, CuK_α line; (b) the transmittance $T(\Theta)$: (*1*) CuK_α and (*2*) CuK_β radiations.

0.0025° and 0.005°, respectively. Option signals were used when working with an asynchronous motor built into the ГУР-8.

TWO-WAVE MEASUREMENT MODE

Reflectivity Measurements

The average density in the surface layer with a thickness of ~10 nm, the period of multilayer structures, and other sample parameters are determined from the shape of the reflectivity $R(\Theta)$ angular dependence measured in the Θ–2Θ scanning mode.

A two-wave reflectometer allows for measuring two curves $R^\alpha(\Theta)$ and $R^\beta(\Theta)$ simultaneously during one angular scanning run. In addition to enhanced measurement efficiency, this makes it possible to achieve more accurate matching between calculated and experimental results by using the recursion relations [6, 7].

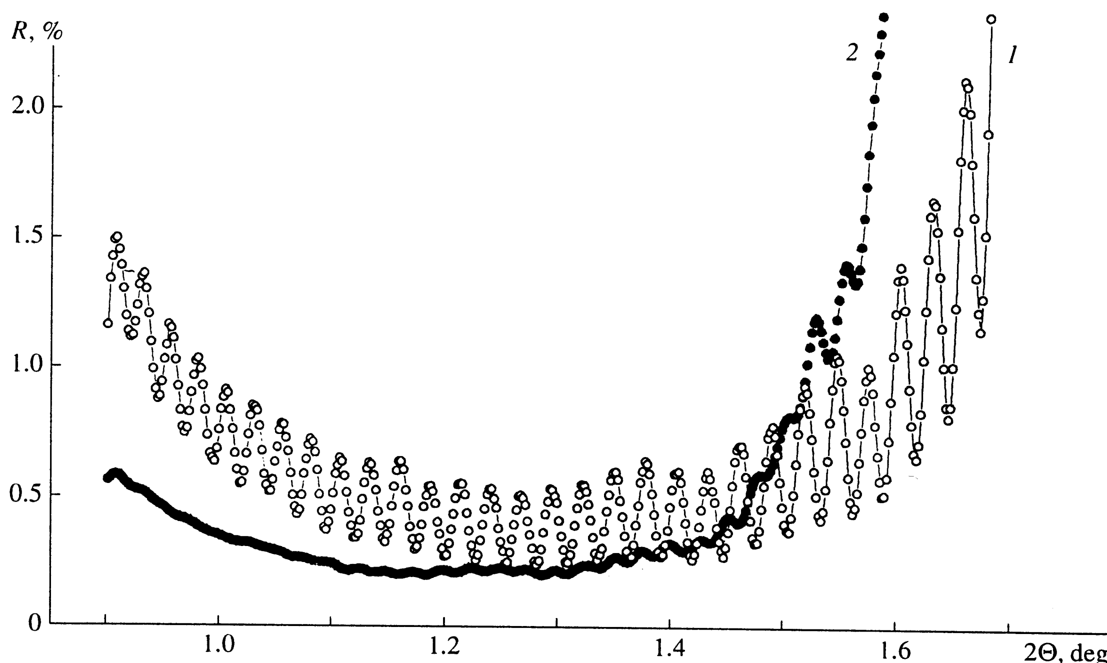

Fig. 4. Angular dependences of the specular reflectivity of a Ni–C multilayer structure: (*1*) CuK_α and (*2*) CuK_β radiations.

Figure 4 shows curves $R(\Theta)$ for a Ni–C multilayer structure on a glass substrate between the critical angle Θ_c of the total external reflection (TER) and the angle of the first Bragg maximum. The period of the structure is $d = 5.16$ nm, the number of periods is 52, and the selected ratio of the Ni layer thickness to the period is $b = 0.25$. The comparison of curves *1* and *2* shows that the $R(\Theta)$ modulation depth caused by subsidiary interference peaks abruptly decreases at a relative change in the radiation wavelength of 10%. This is caused by the K-jump in the Ni absorption for wavelengths between the CuK_α and CuK_β lines, as a result of which the mass absorption coefficient μ increases from 48.5 to 282 cm^{-1} g^{-3}. The obtained data agree with the dependences $R(\Theta)$ calculated with recursion relations. From calculations, it follows that the modulation depth of the curve $R(\Theta)$ depends on the accuracy of preserving the spatial period during deposition of the multilayer structure and on the radiation absorption in the multilayer structure. Since $\mu_{Ni} >> \mu_C$, comparing $R(\Theta)$ for two wavelengths, we can experimentally determine the b value and the probable deviation from the mean d value.

Reflectivity Ratio Measurements

The necessary condition for unambiguous $R(\Theta)$ measurements with a conventional technique is that the reflecting sample surface fully shuts off the incident X-ray beam. For the probe radiation wavelength $\lambda \sim 0.15$ nm, the typical TER critical angle and beam cross-sectional width s are 3.5–5 mrad and 0.1 mm, respectively. The value of s is determined at a level of <0.1 of the intensity distribution maximum in the normal cross section of the incident beam in the zone of the principal axis O_1 of the goniometer. Then, in the case of exact coincidence of the sample surface center with O_1, the beam is fully shut off, if the sample size viewed at the angle Θ exceeds s, i.e., $L\sin\Theta \cong L\Theta > s$ (L is the linear size of the sample in the plane of the X-ray beam incidence). In the considered case, for measurements in an angular range of $(\Theta_c \pm \Theta_c/2)$ at $\Theta_c = 5$ mrad, $L > 40$ mm is necessary. This significantly limits the application of the traditional one-wave reflectometry, because the spatial intensity distribution in the zone of the O_1 axis is not exactly known and $L < 40$ mm is a typical value in complex studies of samples.

Let us consider the possibility of eliminating this difficulty when measuring the ratio of angular dependences of the reflectivities $R^\alpha(\Theta)/R^\beta(\Theta)$ for CuK_α and CuK_β radiations. Note that the selection of other pairs of lines or the use of the reciprocal ratio is not of essential importance.

Under the assumption that the beam is paraxial, at $L\Theta < s$, the measured reflectivity is defined by the expression

$$R_{ex}(\Theta) = \frac{R(\Theta)}{I_0}\int_{x_0-x}^{x_0+x} F(x)dx, \qquad (1)$$

where $R(\Theta)$ is the true reflectivity of the sample; I_0 is the integral intensity of the X-ray beam; x_0 is the sample center position on the coordinate axis x, which lies in the measurement plane, crosses axis O_1, and is per-

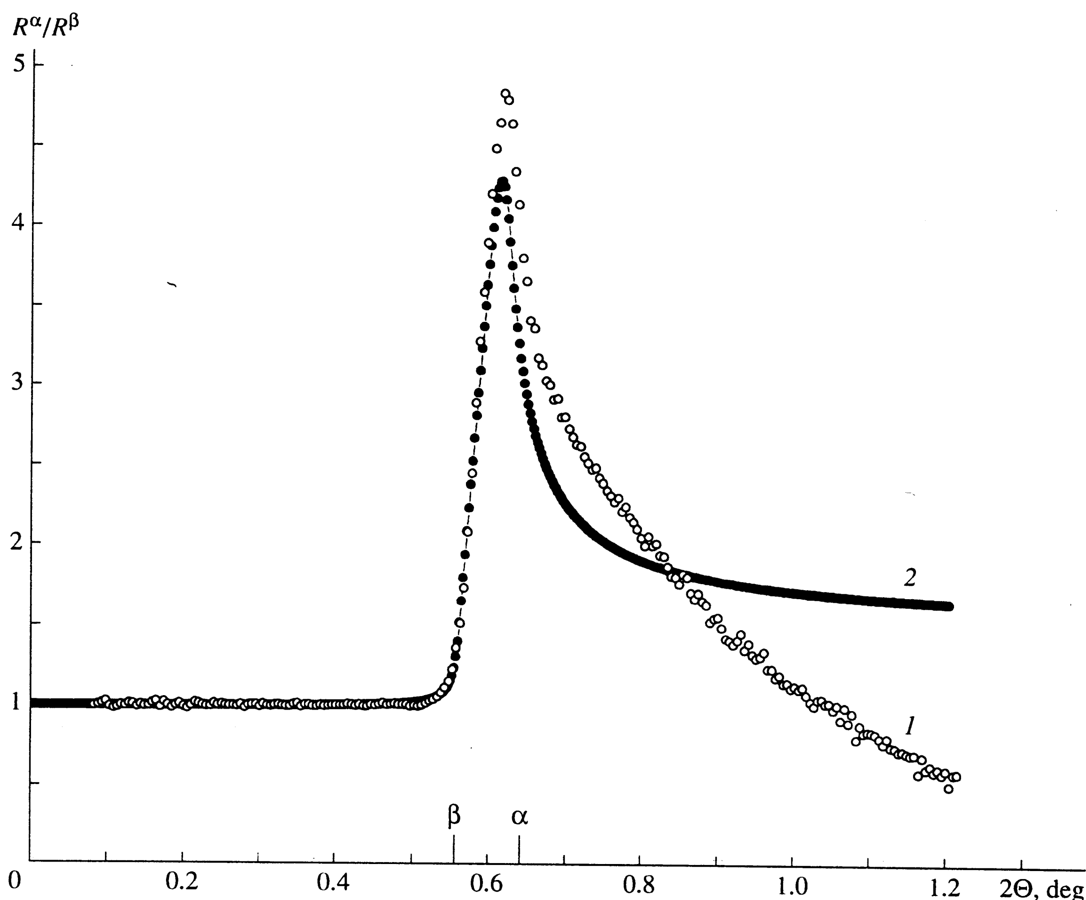

Fig. 5. Angular dependence of the normalized ratio of the specular reflectivities $R^{\alpha}(\Theta)/R^{\beta}(\Theta)$ for a 300-nm-thick GaAs single-crystal film: (*1*) experimental and (2) calculation; α and β are the double critical angles for the CuK_{α} and CuK_{β} lines, respectively.

pendicular to the incident X-ray beam, $x = \Theta L/2$; and $F(x)$ is the X-ray beam intensity distribution function along the x axis. In the general case, $F(x)$ and x_0 are not known exactly, and $F(x)$ depends on the distance between the beam cross section plane and collimator *2* (Fig. 1).

According to the results of measurements, intensity profiles of the direct X-ray beam, which are detected at the CuK_{α} and CuK_{β} lines by scanning the entrance slit *9*, almost coincide. Because, in our scheme, the CuK_{α} and CuK_{β} radiations propagate to the entrance slit in the common transmission channel, it can be assumed that the intensity distribution profiles of the above-mentioned spectral components also coincide in the sample holder zone. Then, when the angular dependences of the reflection intensities are divided by one another, the integral factors in expression (1) are reduced and we derive the angular function $r(\Theta) = gR^{\alpha}(\Theta)/R^{\beta}(\Theta)$, where g is the mere ratio of the integral intensities of the forward beam for the CuK_{α} and CuK_{β} lines and $R^{\alpha}(\Theta)$ and $R^{\beta}(\Theta)$ are the true angular dependences of the reflectivities. Note that $r(\Theta)$ is also independent of temporal changes in the X-ray flux density, which are caused by, for example, X-ray tube current fluctuations or by mechanical shutting-off of a part of the probe beam. As the detected signals decrease, this makes it possible, in particular, to compensate for an increase in statistical counting errors by an increase in the tube current.

A GaAs plate with the size $L = 10$ mm served as a test object for an experimental check of the elimination of measurement errors associated with the effect of the function $F(x)$. At this L, the value of $L\sin\Theta$ is comparable with the beam cross section width within the range of TER angles; i.e., the conditions for direct $R^{\alpha}(\Theta)$ and $R^{\beta}(\Theta)$ measurements are unfavorable. The reflection signal was detected from a 300-nm-thick autoepitaxial GaAs layer grown by the molecular-beam epitaxy technique. The theoretical curve $R^{\alpha}(\Theta)/R^{\beta}(\Theta)$ was calculated on the basis of the reference parameters for GaAs [8, 9]. The results of measurements and calculations are shown in Fig. 5.

In the case of an ideal air–sample interface, the $R^{\alpha}(\Theta)$ and $R^{\beta}(\Theta)$ values must coincide with the reflectivities calculated from the Fresnel formulas [10] for two values of the refractive index n at $\lambda_1 = 0.154$ nm and $\lambda_2 = 0.139$ nm:

$$n(\lambda) = 1 - \delta(\lambda) - i\beta(\lambda), \quad (2)$$

where δ and $i\beta$ are, respectively, the real and imaginary parts of the decrement of the sample material refractive index, which are expressed via the known physical constants and the density and concentration of elements in the near-surface sample layer.

The comparison shows that the theoretical and experimental curves almost coincide over the entire range of grazing incidence angles at $\Theta < \Theta_{c\beta}$; i.e., the error related to an uncontrollable $F(x)$ change is eliminated. In an angular range of $(\Theta_{c\beta}, \Theta_{c\alpha})$, where the effect of the β/δ value on the $R(\Theta)$ profile is significant, the curve $R^{\alpha}(\Theta)/R^{\beta}(\Theta)$ lies higher than that calculated for pure GaAs. This indicates the fact that in this region the ratio $R^{\alpha}(\Theta)/R^{\beta}(\Theta)$ depends on the oxide layer thickness, which is 1–3 nm for GaAs single crystals [11, 12]. For angles $\Theta > \Theta_{c\alpha}$, the experimental ratio $R^{\alpha}(\Theta)/R^{\beta}(\Theta)$ monotonically decreases. This is apparently caused by the interface roughness.

BASIC RESULTS AND CONCLUSIONS

The tests performed have shown that the two-wave X-ray reflectometer has higher metrological characteristics than a one-wave reflectometer and provides new diagnostic capabilities when analyzing near-surface layers.

(1) Higher measurement accuracy, reproducibility, and efficiency are achieved. This is provided by the common transmission channel for radiation propagating from the source to the entrance slit, by the spectral separation just in front of the detecting device, and by the simultaneous data collection at two spectral lines.

(2) Rapid tuning of the reflectometer to an arbitrary spectral line is ensured. A row of semitransparent monochromators provides the basic possibility of simultaneously detecting data in more than two spectral regions. Additional possibilities for increasing the accuracy and sensitivity of the technique are provided in the relative measurement mode.

(3) An essential error of the one-wave scheme for $R(\Theta)$ measurements, which is related to an uncontrollable change in the illumination under the rotation of the reflecting sample surface, is eliminated.

(4) Relative statistical counting errors can be reduced and the dynamic measurement range can be significantly extended by adjusting the X-ray tube current during the data collection procedure.

(5) Limitations for the linear dimensions of the measured sample are canceled, and the operating range of scanning angles is extended.

ACKNOWLEDGMENTS

We are grateful to I.P. Kazakov and E.G. Bugaev for making test samples.

The work was supported by the Russian Foundation for Basic Research (project no. 97-02-17870) and INTAS (project no. 96-0128).

REFERENCES

1. Kozhevnikov, I.V., Asadchikov, V.E., Alaudinov, B.M., *et al., Proc. SPIE-Int. Soc. Opt. Eng.*, 1995, vol. 2453, p. 141.
2. Renner, O., *Czecoslovak J. Phys. B*, 1972, vol. 22, p. 1007.
3. Rietz, R., Rettig, W., Brezensinski, G., *et al., Thin Solid Films*, 1996, vol. 284–285, p. 211.
4. Bilderback, D.H. and Habbard, S., *Nucl. Instrum. Methods Phys. Res.*, 1982, vol. 195, p. 85.
5. Tur'yanskii, A.G., Vinogradov, A.V., and Pirshin, I.V., RF Inventor's Certificate no. 2104481, 1998, MKI G01B 15/08.
6. Parrat, L.G., *Phys. Rev.*, 1954, vol. 95, no. 2, p. 359.
7. Rosenbluth, A.E. and Forsyth, J.M., Abstracts of Papers, *Conf. on Low Energy X-ray Diagnostics*, Monterey, Amer. Inst. Phys., 1981, p. 280.
8. *Sbornik standartov SEMI. Materialy* (Collection of SEMI Standards. Materials), Moscow: ELMA, 1992, vol. 3, p. 205.
9. Henke, B.L., Lee, P., Tanaka, T.J., *et al., At. Data Nucl. Data Tables*, 1982, vol. 27, no. 1, p. 1.
10. Vinogradov, A.V., Brytov, I.A., Grudskii, A.Ya., *et al., Zerkal'naya rentgenovskaya optika* (Mirror X-ray Optics), Moscow: Mashinostroenie, 1989, p. 12.
11. Spring Thorpe, A.J., Ingrei, S.J., Emmerstorfer, B., *et al., Appl. Phys. Lett.*, 1987, vol. 50, no. 2, p. 77.
12. Kohn, E., *J. Electrochem. Soc.: Solid-State Science Techon.*, 1980, vol. 127, no. 2, p. 505.